International Journal of GEOMATE, July, 2017, Vol.13, Issue 35, pp.93-99
Geotec., Const. Mat. & Env., ISSN:2186-2990, Japan, DOI: http://dx.doi.org/10.21660/2017.35.6704

MATHEMATICAL MODELING OF FOREST FIRES INITIATION, SPREAD AND IMPACT ON ENVIRONMENT

*Valeriy Perminov[1] and Alexander Goudov[2]

[1]Department of Ecology Basic Safety, Tomsk Polytechnic University, Russia; [2] Institute of Fundamental sciences, Kemerovo State University, Russia

*Corresponding Author, Received: 08 July 2016, Revised: 01 Dec, 2016, Accepted: 23 Dec. 2016

ABSTRACT: A mathematical model of surface and crown forest fires spread and impact is considered. A three-dimensional multiphase, physic based model is used. The boundary-value problem is solved numerically by finite volume method. This model has been applied to describe the process of initiation and spread of surfaces forest fires and their transfer into crown of forest fires. The results of numerical solutions present the distribution of the main functions of the process (the velocity field, the temperature of gas and solid phase, the concentration of the oxygen, gas product of pyrolysis and inert components, etc.) over time. Scenarios modeled within this study represent a possible approach to the preliminary assessment of risk and should be verified by more detailed computational fluid dynamic (CFD) modeling

Keywords: Crown Fire, Surface Fire, Mathematical Modeling, Finite Volume Method

1. INTRODUCTION

One of the objectives of these studies is the improvement of knowledge on the fundamental physical mechanisms that control forest fires initiation and spread. A great deal of work has been done on the theoretical problem of how forest fire initiation. In forest, there are two steps for crown forest fire initiation: spread of fire from crow to crown and crown fires are initiated by convective and radiative heat transfer from surface fires. However, convection is the main heat transfer mechanism. Firstly, crown forest fire initiation has been studied and modeled by Van Wagner [1]. There are three simple crown properties: crown base height, bulk density and moisture content of forest fuel in this theory. Also, crown fire initiation has been studied and modeled in detail (eg: Alexander [2], Van Wagner [3], Xanthopoulos, [4], Rothermel [5,6], Van Wagner, [7], Cruz [8], Albini [9], Scott, J. H. and Reinhardt, E. D. [10]. The discussion of the problem of modeling forest fires is provided by a group of co-workers at Tomsk University (Grishin [11], Grishin and Perminov [12]. The general mathematical model of forest fires was obtained by Grishin [11] based on an analysis of known and original experimental data [11,13], and using concepts and methods from reactive media mechanics. The physical two-phase models used in [14-15] may be considered as a continuation and extension of the formulation proposed by Grishin and Perminov [12]. However, the investigation of crown fires has been limited mainly to cases studied of forest fires initiation in two dimensional settings and did not take into account space properties of these phenomena.

2. PHYSICAL AND MATHEMATICAL MODEL

It is assumed that the forest during a forest fire can be modeled as 1) a multi-phase, multistoried, spatially heterogeneous medium; 2) in the fire zone the forest is a porous-dispersed, two-temperature, single-velocity, reactive medium; 3) the forest canopy is supposed to be non-deformed medium (trunks, large branches, small twigs and needles), affects only the magnitude of the force of resistance in the equation of conservation of momentum in the gas phase, i.e., the medium is assumed to be quasi-solid (almost non-deformable during wind gusts); 4) let there be a so-called "ventilated" forest massif, in which the volume of fractions of condensed forest fuel phases, consisting of dry organic matter, water in liquid state, solid pyrolysis products, and ash, can be neglected compared to the volume fraction of gas phase (components of air and gaseous pyrolysis products); 5) the flow has a developed turbulent nature and molecular transfer is neglected; 6) gaseous phase density doesn't depend on the pressure because of the low velocities of the flow in comparison with the velocity of the sound. Let the coordinate reference point x_1, x_2 , x_3= 0 (Figure 1) be situated

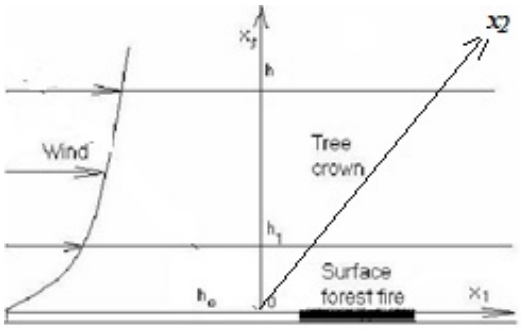

Fig.1. Schematic of a forest fire domain

at the center of the domain of surface forest fire source at the height of the roughness level, axis $0x_1$ directed parallel to the Earth's surface to the right in the direction of the unperturbed wind speed, axis $0x_2$ directed perpendicular to $0x_1$ and axis $0x_3$ directed upward. Using the results of [11-12] and known experimental data [13] we have the following sufficiently general equations, which define the state of the medium in the forest fire zone, written using tensor notation.

$$\frac{\partial \rho}{\partial t}+\frac{\partial}{\partial x_j}(\rho v_j)=\dot{m},\ j=1,2,3,\ i=1,2,3; \quad (1)$$

$$\rho\frac{dv_i}{dt}=-\frac{\partial P}{\partial x_i}+\frac{\partial}{\partial x_j}(-\rho\overline{v_i'v_j'})-\rho s c_d v_i|\vec{v}|- \quad (2)$$
$$-\rho g_i-\dot{m}v_i;$$

$$\rho c_p\frac{dT}{dt}=\frac{\partial}{\partial x_j}(-\rho c_p\overline{v_j'T'})+q_5R_5-\alpha_v(T-T_s)+ \quad (3)$$
$$+k_g(cU_R-4\sigma T^4)$$

$$\rho\frac{dc_\alpha}{dt}=\frac{\partial}{\partial x_j}(-\rho\overline{v_j'c_\alpha'})+R_{5\alpha}- \quad (4)$$
$$-\dot{m}c_\alpha\ ,\ \alpha=\overline{1,3};$$

$$\frac{\partial}{\partial x_j}\left(\frac{c}{3k}\frac{\partial U_R}{\partial x_j}\right)-kcU_R+4k_S\sigma T_S^4+ \quad (5)$$
$$+4k_g\sigma T^4=0, k=k_g+k_S,$$

$$\sum_{i=1}^{4}\rho_i c_{pi}\varphi_i\frac{\partial T_S}{\partial t}=k_s(cU_R-4\sigma T_S^4)+ \quad (6)$$
$$+q_3R_3-q_2R_2+\alpha_V(T-T_S);$$

$$\rho_1\frac{\partial\varphi_1}{\partial t}=-R_1,\rho_2\frac{\partial\varphi_2}{\partial t}=-R_2, \quad (7)$$
$$\rho_3\frac{\partial\varphi_3}{\partial t}=\alpha_C R_1-\frac{M_C}{M_1}R_3,\rho_4\frac{\partial\varphi_4}{\partial t}=0;$$

$$\sum_{\alpha=1}^{3}c_\alpha=1,\ p_e=\rho RT\sum_{\alpha=1}^{3}\frac{c_\alpha}{M_\alpha},\vec{v}=(v_1,v_2,v_3).$$

The system of equations (1)–(7) must be solved taking into account the initial and boundary conditions

$$t=0: v_1=0, v_2=0, v_3=0, T=T_e, c_\alpha=c_{\alpha e}, \quad (8)$$
$$T_s=T_{se}, \varphi_i=\varphi_{ie};$$

$$x_1=-x_{1e}: v_1=V_e, v_2=0, v_3=0, T=T_e, c_\alpha=c_{\alpha e}, \quad (9)$$
$$-\frac{c}{3k}\frac{\partial U_R}{\partial x_1}+\frac{c}{2}U_R=0,$$

$$x_1=x_{1e}:\frac{\partial v_1}{\partial x_1}=0,\ \frac{\partial v_2}{\partial x_1}=0,\frac{\partial v_3}{\partial x_1}=0,\ \frac{\partial c_\alpha}{\partial x_1}=0, \quad (10)$$
$$\frac{\partial T}{\partial x_1}=0,\frac{c}{3k}\frac{\partial U_R}{\partial x_1}+\frac{c}{2}U_R=0;$$

$$x_2=x_{20}:\frac{\partial v_1}{\partial x_2}=0,\ \frac{\partial v_2}{\partial x_2}=0,\ \frac{\partial v_3}{\partial x_2}=0,\frac{\partial c_\alpha}{\partial x_2}=0, \quad (11)$$
$$\frac{\partial T}{\partial x_2}=0,-\frac{c}{3k}\frac{\partial U_R}{\partial x_2}+\frac{c}{2}U_R=0;$$

$$x_2=x_{2e}:\frac{\partial v_1}{\partial x_2}=0,\ \frac{\partial v_2}{\partial x_2}=0,\frac{\partial v_3}{\partial x_2}=0,\frac{\partial c_\alpha}{\partial x_2}=0, \quad (12)$$
$$\frac{\partial T}{\partial x_2}=0,\frac{c}{3k}\frac{\partial U_R}{\partial x_2}+\frac{c}{2}U_R=0.$$

$$x_3=0: v_1=0,\ v_2=0,\frac{\partial c_\alpha}{\partial x_3}=0,-\frac{c}{3k}\frac{\partial U_R}{\partial x_3}+\frac{c}{2}U_R=0, \quad (13)$$
$$v_3=v_{30}, T=T_g, |x_1|\le\Delta, |x_2|\le\Delta$$
$$v_3=0,\ T=T_e, |x_1|>\Delta, |x_2|>\Delta;$$

$$x_3=x_{3e}:\frac{\partial v_1}{\partial x_3}=0,\ \frac{\partial v_2}{\partial x_3}=0,\frac{\partial v_3}{\partial x_3}=0,\frac{\partial c_\alpha}{\partial x_3}=0, \quad (14)$$
$$\frac{\partial T}{\partial x_3}=0,\frac{c}{3k}\frac{\partial U_R}{\partial x_3}+\frac{c}{2}U_R=0.$$

Here and above $\frac{\mathrm{d}}{\mathrm{d}t}$ is the symbol of the total (substantial) derivative:

$\frac{d}{dt}=\frac{\partial}{\partial t}+v_1\frac{\partial}{\partial x_1}+v_2\frac{\partial}{\partial x_2}+v_3\frac{\partial}{\partial x_3}$, α_V is the coefficient of phase exchange; ρ - density of gas – dispersed phase, t is time; v_i - the velocity components; T, T_S, - temperatures of gas and solid phases, U_R - density of radiation energy, k - coefficient of radiation attenuation, P - pressure; c_p – constant pressure specific heat of the gas phase, c_{pi}, ρ_i, φ_i – specific heat, density and volume of fraction of condensed phase (1 – dry organic substance, 2 – moisture, 3 – condensed pyrolysis products, 4 – mineral part of forest fuel), R_i – the mass rates of chemical reactions, q_i – thermal effects of chemical reactions; k_g , k_S - radiation absorption coefficients for gas and condensed phases; T_e - the ambient temperature; c_α - mass concentrations of α - component of gas - dispersed medium, index α=1,2,3, where 1 corresponds to the density of oxygen, 2 - to carbon monoxide *CO*, 3 - to carbon dioxide and inert components of air; R – universal gas constant; M_α , M_C, and M molecular mass of α -components of the gas phase, carbon and air mixture; g is the gravity acceleration; c_d is an empirical coefficient of the resistance of the vegetation, s is the specific surface of the forest fuel in the given forest stratum. To define source terms which characterize inflow (outflow of mass) in a volume unit of the gas-dispersed phase, the following formulae were used for the rate of formulation of the gas-dispersed mixture $\dot{m}$, outflow of oxygen R_{51} and

changing carbon monoxide R_{52}.

$$\dot{m} = (1-\alpha_c)R_1 + R_2 + \frac{M_c}{M_1}R_3,$$

$$R_{51} = -R_5 - \frac{M_1}{2M_2}' R_{52} = \nu_g(1-\alpha_c)R_1 - R_5, R_{53} = 0,$$

$$R_1 = k_1\rho_1\varphi_1 \exp(-\frac{E_1}{RT_S}), R_2 = k_2\rho_2\varphi_2 T^{-0.5}\exp(-\frac{E_2}{RT_S}),$$

$$R_3 = k_3\rho\varphi_3 S_\sigma c_1 \exp(-\frac{E_3}{RT_S}),$$

$$R_5 = k_5 M_2\left(\frac{c_1 M}{M_1}\right)^{0.5}\left(\frac{c_2 M}{M_2}\right)T^{-2.25}\exp(-\frac{E_5}{RT}).$$

The initial values for volume of fractions of condensed phases are determined using the expressions:

$$\varphi_{1e} = \frac{d(1-\nu_z)}{\rho_1}, \varphi_{2e} = \frac{Wd}{\rho_2}, \varphi_{3e} = \frac{\alpha_c\varphi_{1e}\rho_1}{\rho_3}.$$

where d -bulk density of forest combustible materials, ν_z – coefficient of ashes of forest fuel, W – forest fuel moisture content. It is supposed that the optical properties of a medium are independent of radiation wavelength (the assumption that the medium is "grey"), and the so-called diffusion approximation for radiation flux density were used for a mathematical description of radiation transport during forest fires. To close the system (1)–(7), the components of the tensor of turbulent stresses, and the turbulent heat and mass fluxes are determined using the local-equilibrium model of turbulence (Grishin, [1]. Processes of transfer within the entire region of the forest massif, which includes the space between the underlying surface and the base of the forest canopy, the forest canopy and the space above it, while the appropriate components of the data base are used to calculate the specific properties of the various forest strata and the near-ground layer of atmosphere. This approach substantially simplifies the technology of solving problems of predicting the state of the medium in the fire zone numerically. The thermodynamic, thermophysical and structural characteristics correspond to the forest fuels in the canopy of a different (for example pine [10,12]) type of forest

3. NUMERICAL SOLUTION AND REZULTS

The boundary-value problem (1)–(7) we solve numerically using the method of splitting according to physical processes [12]. In the first stage, the hydrodynamic pattern of flow and distribution of scalar functions was calculated. The system of ordinary differential equations of chemical kinetics obtained as a result of splitting [12] was then integrated. A discrete analog was obtained by means of the control volume method using the SIMPLE like algorithm [12,16,17]. The accuracy of the program was checked by the method of inserted analytical solutions. The time step was selected automatically. Fields of temperature, velocity, component mass fractions, and volume fractions of phases were obtained numerically. Figure 2 illustrate the time dependence of dimensionless temperatures of gas (1) and condensed phases (2), Figure 3. – mass concentrations of gas components (1- oxygen, 2- gas products of pyrolysis), and Fig.4 - relative volume fractions of solid phases (1), moisture (2) and coke (3) at crown base of the forest (V_e=5m/s). At the moment of ignition, the gas combustible products of pyrolysis burn away, and the concentration of oxygen is rapidly reduced. The temperatures of both phases reach a maximum value at the point of ignition. The ignition processes are of a gas - phase nature, i.e. initially heating of solid and gaseous phases occurs, moisture is evaporated. Then decomposition process into condensed and volatile pyrolysis products starts, the latter being ignited in the forest canopy.

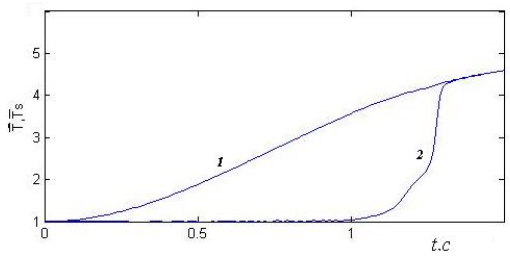

Fig.2 Temperature of gas (1 - $\bar{T}$) and solid phase (2 - $\bar{T}_S$); $\bar{T} = T/T_e$, $\bar{T}_S = T_S/T_e$, T_e=300K

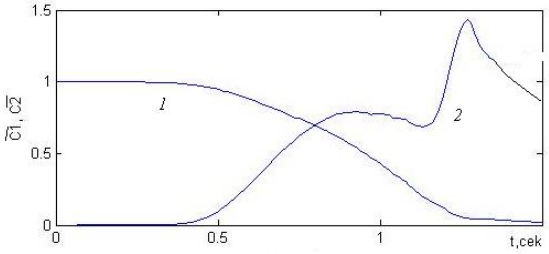

Fig.3 Concentration of oxygen (1- $\bar{C}_1$) and gas products of pyrolysis (2 - $\bar{C}_2$); $\bar{c}_\alpha = c_\alpha / c_{1e}, c_{1e} = 0.23$.

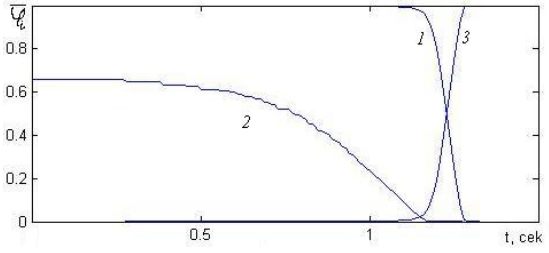

Fig.4 Volume fractions of solid phase: $1 - \bar{\varphi}_1 = \varphi_1 / \varphi_{1e}, 2 - \bar{\varphi}_2 = \varphi_2 / \varphi_{2e}, 3 - \bar{\varphi}_3 = \varphi_3 / \varphi_{3e}$.

The vector field of velocities and isotherms of gas phase (Fig. 5): 1-6 correspond to the isotherms $\overline{T}$ = 1.1, 1.5, 1.7, 2, 3 and 4. In the vicinity of the source of heat and mass release, heated air masses and products of pyrolysis and combustion float up. The wind field in the forest canopy interacts with the gas-jet obstacle that forms from the surface forest fire source and from the ignited forest canopy base. Recirculating flow forms beyond the zone of heat and mass release, while on the windward side the movement of the air flowing past the ignition region accelerates. Under the influence of the wind the tilt angle of the flame is increased. As a result, this part of the forest canopy, which is shifted in the direction of the wind from the center of the surface forest fire source, is subjected to a more intensive warming up. The isotherms of the gas and condensed phases are deformed in the direction of the wind.

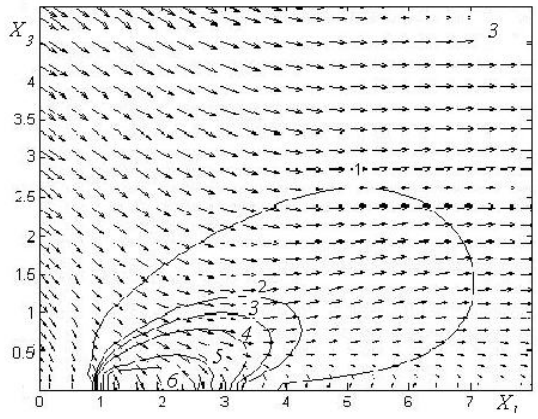

Fig.5. The vector field of velocities and isotherms of gas phase; (*t*=4 sec.)

Figure 6 presents isolines of oxygen for different instants of time (*t*=2, 3, 4 sec.): 1-5 correspond to the isolines $\overline{c}_1$ = 0.9, 0.8, 0.7, 0.5 and 0.1. Figure 7 presents isolines of gas products of pyrolysis: 1-4 correspond to the isolines $\overline{c}_2$ = 0.02, 0.05, 0.1 and 0.5.

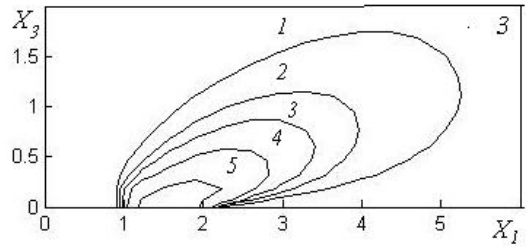

Fig.6 Isolines of oxygen (*t*= 4 sec.)

At $V_e \neq 0$ the forest fire source ignites the forest crown and burn away in the forest canopy. Forest fire begins to spread in the forest canopy. The distribution of temperature, concentrations of gas products of pyrolysis and oxygen in the

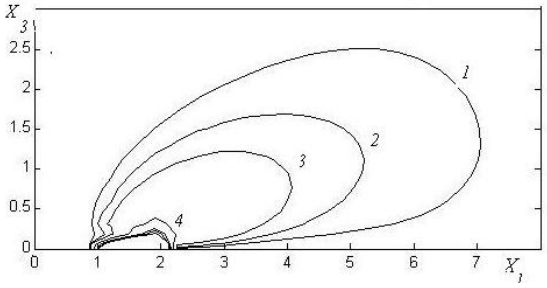

Fig.7. Isolines of gas products of pyrolysis (*t*=4 sec.)

forest fire front are presented in the Figure 8. It is seen that the combustion wave looks like as a soliton. The oxygen concentration drops to near zero in front of a fire. It is consumed in the combustion of the pyrolysis products, the concentration of which is reached their maximum before the maximum of temperature. Figures 9 - 10 present the distribution of temperature $\overline{T}$ ($\overline{T} = T/T_e, T_e = 300K$) (1- 1.5, 2 - 2., 3 – 2.6, 4 – 3, 5 – 3.5, 6 – 4.) for gas phase, concentrations of oxygen $\overline{c}_1$ (1 – 0.1, 2 – 0.5, 3 – 0.6, 4 – 0.7, 5 – 0.8, 6 – 0.9) and volatile combustible products of pyrolysis $\overline{c}_2$ (1 – 1., 2- 0.1, 3 – 0.05, 4 – 0.01) ($\overline{c}_\alpha = c_\alpha / c_{1e}, c_{1e} = 0.23$) at different instants of time for wind velocity V_e= 5 m/s (Fig.9) and V_e= 10 m/s (Fig.10).

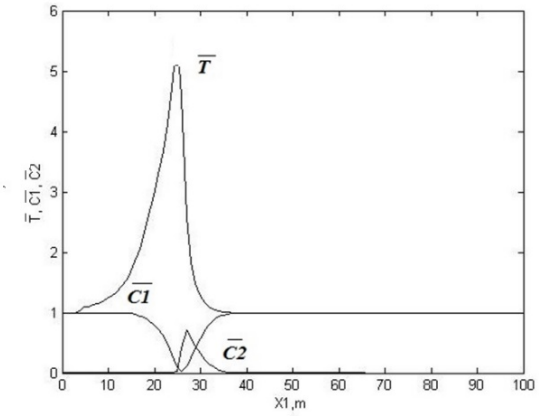

Fig.8 The distribution of gas temperature, concentrations of gas products of pyrolysis and oxygen

The distribution of isotherms of combustion temperature shows the moving of forest fire front with time. Figure 10 shows that with the increase of wind speed up to 10 m/s

increases the rate of fire spread to 5 m/sec. Ignition of forest due to spotting is one of the most difficult aspects to understand the behavior of fires. The phenomenon of spotting fires comprises three sequential mechanisms: generation, transport and ignition of recipient fuel. The present mathematical model and results of calculation are used to illustrate picture of the formation of large fires by combining small combustion sources arising from the transfer of firebrands. In order to understand these mechanisms, many calculation experiments have been performed. In the Figures 11 - 12 the process of formation large forest fire front as a result of integration of various sources of combustion is showed. The distributions of temperature for gas phase(a), concentrations of oxygen (b) and volatile combustible products of pyrolysis (c) at different times (I - t=3 sec., II - t=6 sec, III - t=12 sec.) for *Ve*= 5 m/s are presented. There are present the same values of isotherms and isolines of concentration for and as well as in the Figures 11-12. If the sources of ignition from the burning particles are arranged in a triangle, the processes of formation of the forest fire front are shown in Figures 11-12. In the second case (Figure 12), the right ignition source in the x_2 direction was 2 times less than in the first case (Figure 11).

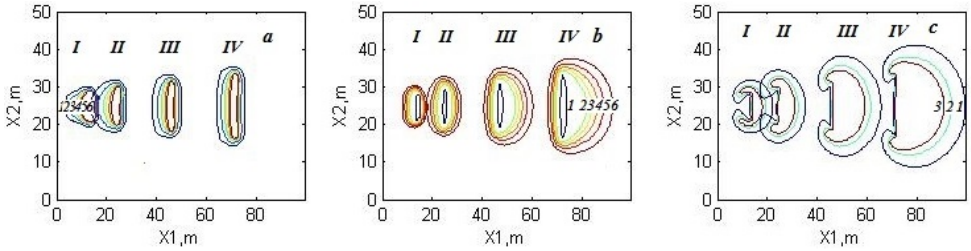

Fig. 9 The distribution of *a*) temperature for gas phase, *b)* concentration of oxygen and c) volatile combustible products of pyrolysis; V_e= 5 m/s, at different instants of time: I - t=3 sec., II - t=6 sec, III - t=12 sec., IV - t= 20 sec.

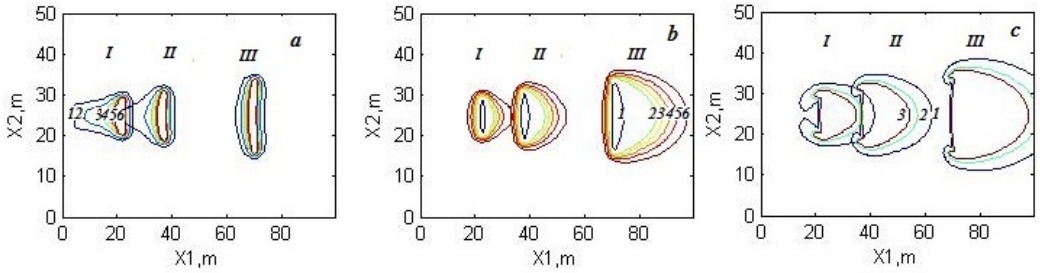

Fig.10 The distribution of *a*) temperature for gas phase, *b)* concentrations of oxygen and c) volatile combustible products of pyrolysis; V_e= 10 m/s, at different instants of time: I - t=3 sec., II - t=6 sec, III - t=12 sec., IV - t= 20 sec.

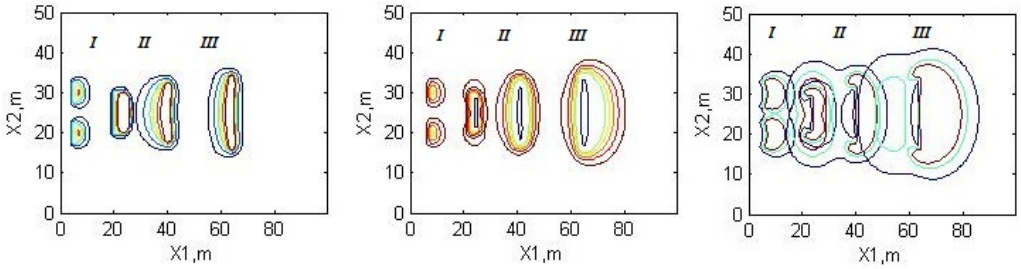

Fig. 11. The distribution of temperature, concentrations of oxygen and volatile combustible products of pyrolysis.

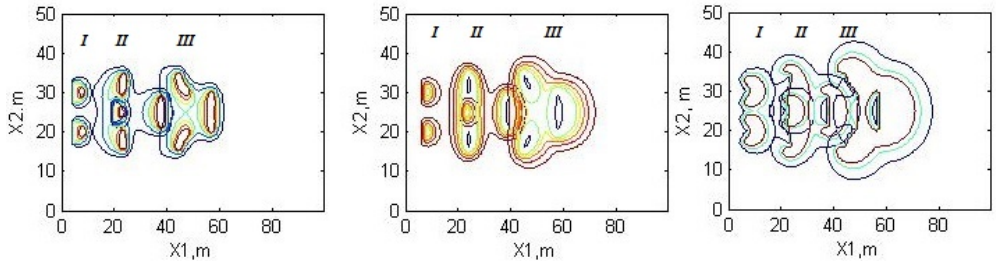

Fig. 12. The distribution of temperature, concentrations of oxygen and volatile combustible products of pyrolysis.

4. CONCLUSION

Results of calculation give an opportunity to describe the different conditions of the forest fire spread taking account different weather conditions and state of forest combustible materials, which allows applying the given model for prediction and preventing fires. It overestimates the rate of crown forest fire spread that depends on crown properties: bulk density, moisture content of forest fuel, wind velocity and etc. The model proposed here gives a detailed picture of the change in the temperature and component concentration fields with time, and determine as well as the influence of different conditions on the crown forest fire spreading for the different cases of inhomogeneous of distribution of sources of forest fires initiation.

5. ACKNOWLEDGEMENTS

This research was financially supported by the Russian Foundation for Basic Research in 2016 (the project № 16-41-700022 p_a) and on the state task № 2014/64, the state project "Scientific researches organization".

6. REFERENCES

1. Van Wagner CE, Conditions for the start and spread of crown fire, Canadian Journal of Forest Research, Vol. 7, 1977, pp. 23-34.
2. Alexander ME, "Crown fire thresholds in exotic pine plantations of Australasia", PhD thesis, Department of Forestry, Australian National University, Australia, 1998.
3. Van Wagner CE, Prediction of crown fire behavior in conifer stands, Proc. '10th conference on fire and forest meteorology. Ottawa, Ontario. (Eds D. C. MacIver, H. Auld and R. Whitewood), 1989, pp. 207-212.
4. Xanthopoulos G., Development of a wildland crown fire initiation model, PhD thesis, University of Montana, USA, 1990.
5. Rothermel RC. Crown fire analysis and interpretation, Proc. International conference on fire and forest meteorology. Missoula, Montana, USA, 1991.
6. Rothermel RC, Predicting behavior of the 1988 Yellowstone Fires: projections versus reality, Int. Journal of Wildland Fire, Vol. 1, 1991, pp. 1-10.
7. Van Wagner CE, Prediction of crown fire behavior in two stands of jack pine, Canadian Journal of Forest Research, Vol. 23, 1999, pp. 445-449.
8. Cruz MG, Predicting crown fire behavior to support forest fire management decision-making, Proc. IV International conference on forest fire research, Luso-Coimbra, Portugal. (Ed. D. X. Viegas), 11 [CD-ROM]. (Millpress), 2002.
9. Albini FA, Modeling ignition and burning rate of large woody natural fuels, Int. Journal of Wildland fire, vol. 5, 1995, pp. 81-91.
10. Scott JH, Assessing crown fire potential by linking models of surface and crown fire behavior, USDA Forest Service, Rocky Mountain Forest and Range Experiment Station. Fort Collins: RMRS-RP-29, (Colorado, USA), 2001.
11. Grishin AM, Mathematical Modeling Forest Fire and New Methods Fighting Them, Publishing House of Tomsk University, Tomsk, Russia, 1997.
12. Grishin AM, Perminov VA, "Mathematical modeling of the ignition of tree crowns", Combustion, Explosion, and Shock Waves, Vol. No 34, 1998, pp. 378-386.
13. Konev EV, The physical foundation of vegetative materials combustion, Nauka, Novosibirsk, Russia, 1977.
14. Morvan D, Dupuy JL, "Modeling of fire spread through a forest fuel bed using a multiphase formulation", Combustion and Flame, Vol. 127, 2001, pp. 1981-1994.
15. Morvan D, Dupuy JL, "Modeling the propagation of wildfire through a Mediterranean shrub using a multiphase formulation", Combustion and Flame, Vol. 138, 2004, pp. 199-210.
16. Patankar SV, Numerical Heat Transfer and Fluid Flow, Hemisphere Publishing Corporation, New York, 1981.
17. Goudov AM, Perminov VA, Mathematical Simulation of Contaminant Flow in the Square Closed Reservoir, International Journal of Geomate, Vol.11, No 26, 2016, pp.2558-2562.